Appl. Phys. A 61, 645–649 (1995)

Applied Physics A Materials Science & Processing

Cathodoluminescence microscopic studies of α-HgI_2 platelets and crystals

U. Pal[1], J. Piqueras[1], M.D. Serrano[2], N.V. Sochinski[2–4], E. Diéguez[2]

[1] Departmento de Física de Materiales, Facultad de Ciencias Físicas, Universidad Complutense, E-28040 Madrid, Spain (Fax: + 34-1/3944547)
[2] Departmento de Física de Materiales, Universidad Autónoma, Cantoblanco-Madrid, E-28049 Madrid, Spain
[3] Institute of Semiconductor Physics, Pr. Nauki 45, 252650 Kiev, Ukraine
[4] New Semiconductor Inc., P.O. Box 222, 254210 Kiev, Ukraine

Received: 1 December 1994/Accepted: 18 February 1995

Abstract. CathodoLuminescence studies (CL) have been carried out on red mercuric-iodide (α-HgI_2) crystals and platelets grown by the vapor transport method. Panchromatic CL images revealed inhomogeneous distribution of growth-induced dislocations and terraces. The effect of prolonged KI (20%) treatment on the evolution of different CL bands has been investigated. CL spectra of the platelets at 80 K showed three luminescence bands at about 546, 567 and 624 nm. The intensity of the 567 nm band (band II) decreased after KI treatment, thus indicating the role of I vacancies on the evolution of this band. An additional band at about 555 nm is observed in as-grown crystals, but not revealed in platelets. Increase of the relative intensity of band III (624 nm) on prolonged KI treatment indicates the association of some surface states on this band along with the effect of impurities as reported earlier. Hg treatment causes an increase of total CL intensity and also the relative intensity of band II in platelets and crystals.

PACS: 71.55.Gs; 78.60.Hk

The red mercuric iodide (α-HgI_2) is a high-Z compound and a high resistive material, which has attracted considerable attention for its potential applications in room temperature X-ray and gamma-ray detectors and spectrometers [1–4]. However, the performance of HgI_2 detectors varies widely, and material from a particular source crystal may produce detectors of different grades [5]. This is due to native defects and impurities introduced during crystal growth. For this reason, the characterization of defects in HgI_2 and the determination of their effects on the electronic properties are of great interest. Although a number of workers have employed the Photo-Luminescence (PL) technique to correlate the luminescence features with detector performance [6, 7], impurities [6, 8] and stoichiometry [6, 7], the exact interpretation of various luminescence bands is still under open discussion. Studies of microstructure in HgI_2 have previously been carrried out using optical microsocpy [9] and Scanning Electron Microscopy (SEM) with secondary electron imaging techniques [10]. However, there are very few reports [9, 11, 12] on the spectroscopic CathodoLuminescence (CL) studies on the HgI_2 crystals so far.

In the present work, CL in SEM is used to study defects in HgI_2 platelets and crystals. The effect of surface treatment with 20% (weight) KI solution and Hg on the evolution of different luminescence bands has been studied. CL imaging technique has been used to visualize the different electrically active defects in HgI_2 platelets and crystals.

1 Experiments

HgI_2 platelets of about $6 \times 4 \times 0.1$ mm [13] and crystals of about $15 \times 10 \times 10$ mm dimensions were grown by the physical vapor transport method. The crystals were cut to slices of about $10 \times 10 \times 1$ mm by a wire saw dipped in 20% KI solution and used for CL studies. The crystallographic orientation of crystals and platelets was (0 0 1). The samples were observed in a Hitachi S-2500 scanning electron microscope in emissive and CL modes at 80 K with an accelerating voltage of 10 keV. The experimental setup for spectral and panchromatic CL measurements with a Thorn EMI B2F photomultiplier tube has been previously described [14]. Some of the samples (both platelets and crystals) were treated by 20% (weight) KI solution (aquas) for 2 min and kept under atmospheric conditions without cleaning. As the samples were not cleaned/washed after etching, the reaction of KI with the samples continued for several days. The CL spectra and images were taken before KI treatment, immediate after KI treatment and after several days of KI treatment. Some of the samples were treated with Hg by keeping them in a Hg bath for several days.

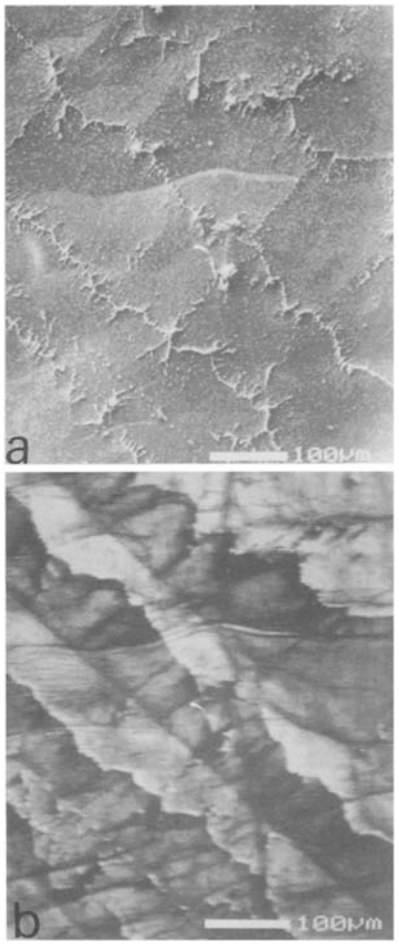

Fig. 1. a Secondary and **b** CL images of a typical part of as-grown platelet. Growth-instability-induced terraces and grooves can be seen

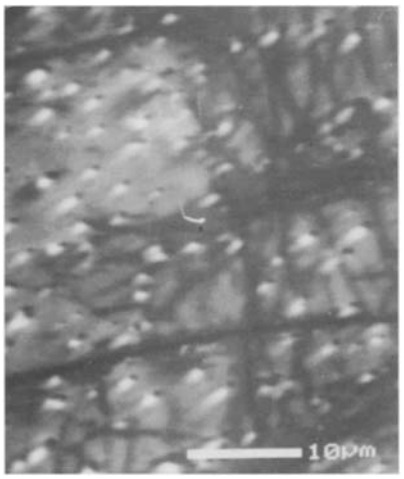

Fig. 2. CL image of as-grown platelet showing Hg droplets appearing black. The brighter tails associated with each of the Hg droplets may be due to segregation of impurities at the shadowed part

2 Results

Microscopic observations of the platelets revealed different features at different places of the samples. Figure 1a and b shows the images of a particular place of platelet in secondary mode and CL mode, repectively. Emissive mode images show a surface relief in platelets and a smooth surface in the case of crystals. CL images show an inhomogeneous emission with an array of dark lines in some regions of the samples. In Fig. 1b the array of wavy lines appears sometimes crossed by sets of straight lines. In Fig. 2 the magnified CL image of a place of platelets is shown which appeared smooth in emissive mode. Along with some homogeneous distribution of black dots with a bright halo, some black lines were observed. In the case of crystals, generally a smooth surface was observed in emissive mode. In CL mode some black dots appear (Fig. 3), possibly related to the presence of forest dislocations [11].

In Fig. 4 the CL image of a particular place of the crystal is shown. An array of dark lines on a brighter background appears and sometimes crossed by sets of straight lines. Figure 5 shows a typical CL image of HgI_2 crystal immediately after KI treatment.

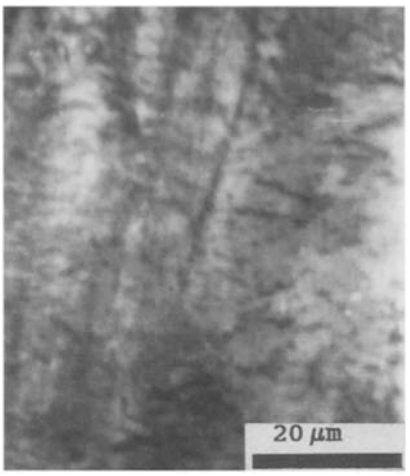

Fig. 3. CL image of as-grown crystal showing forest-like dislocations

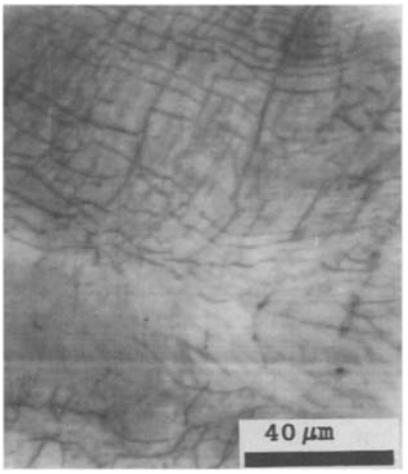

Fig. 4. CL image of a typical place of as-grown crystals showing basal plane dislocation

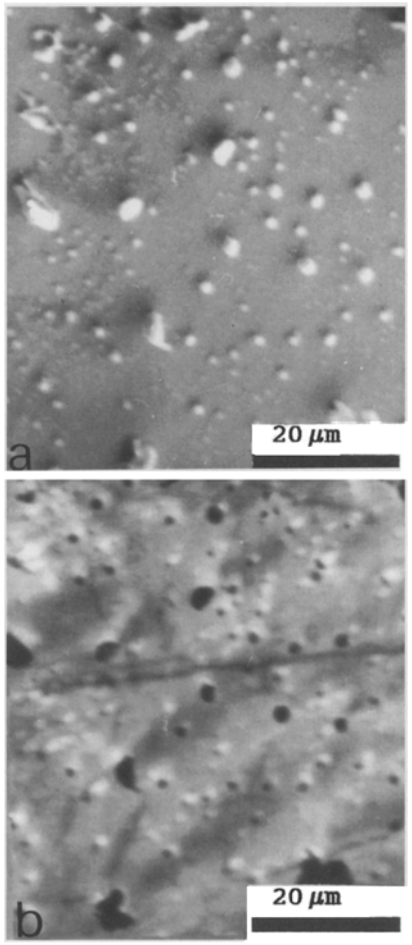

Fig. 5a, b. Typical **a** secondary and **b** CL image of HgI_2 crystal immediately after KI treatment

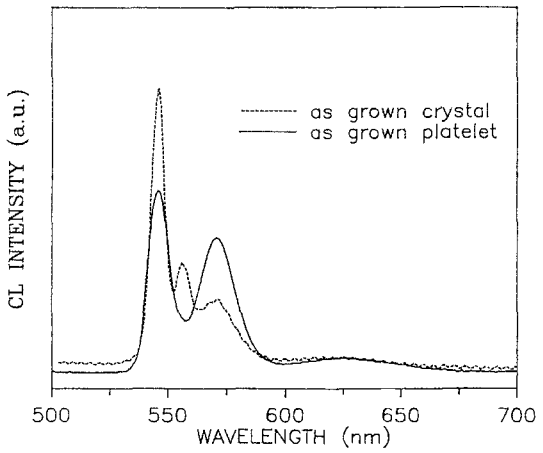

Fig. 6. CL spectra of as-grown platelet and as-grown crystal

CL spectra of untreated platelets show three emission bands which have been previously reported. Band I, centered at about 546 nm, corresponds to near band gap emission. Bands II and III are centered at about 567 and 624 nm, respectively. Spectra of untreated/as-grown crystals show an additional band at about 555 nm while band II is almost absent. Figure 6 shows representative spectra of as-grown platelets and crystals. Some of the samples were etched and subsequently kept in air without cleaning. This treatment causes in the platelets a complex evolution of CL bands (Fig. 7). Immediately after etching, the samples show a reduced CL intensity. The relative decrease of intensity is more pronounced for band II and this effect is enhanced with increasing exposure time. In Fig. 8 a plot of relative intensity (I_2/I_1) for band II with exposure time is plotted. Although the relative intensity of band II was found to decrease even after several days of etching, it increased again after about 10 days. However, the plot of relative intensity (I_3/I_1) of band III shows just opposite behavior to band II.

Figure 9 shows the CL spectrum of a crystal immediately after KI treatment, in which only the luminescence in the fundamental region is pronounced.

Treatment with Hg also affects luminescence efficiency. However, the exact behavior depends on the kind of sample and on the sample region. Clear changes have been observed in platelets, which show increased luminescence with relative increase of band II after Hg treatment.

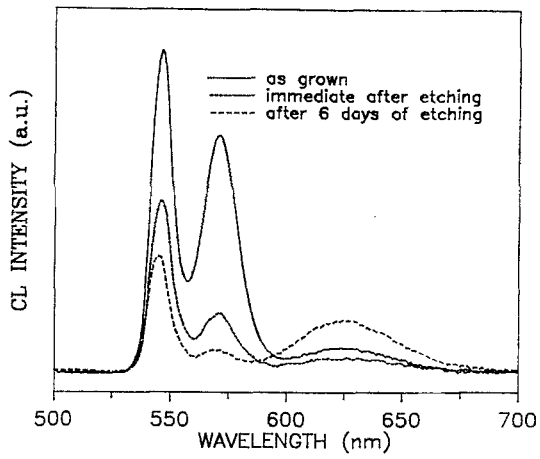

Fig. 7. CL spectra of HgI_2 platelets before KI treatment, immediately after KI treatment, and after 6 days of KI treatment

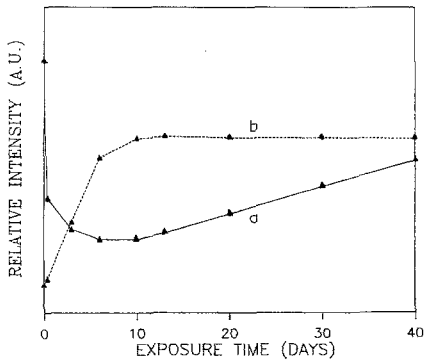

Fig. 8. Plots of relative intensity (I_i/I_1) of *a* band II and *b* band III emissions with exposure time

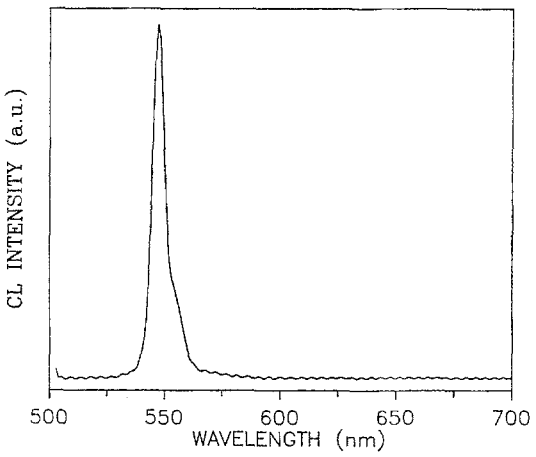

Fig. 9. CL spectrum of HgI_2 crystal immediately after KI treatment

3 Discussion

Figures 1 and 2 show characteristic emissive mode and CL images of the platelets. Although the observations at different places of the platelets revealed different structure, a general surface relief with cellular structure is observed in emissive mode almost all over the places of the platelets. The boundaries of the subgrains appeared brighter in emissive mode and dark in CL mode. From the images it appears that the sub-boundaries are decorated by fine Hg droplets. The appearance of terraces like steps well visualized in Fig. 1b is related to growth process along a direction in the (0 0 1) plane, leading to the formation of grooves.

Some superficial decomposition of HgI_2 occurs, leading to the formation of small Hg droplets (Fig. 2). The Hg droplets show a bright contrast in SE, but appear dark in CL. A similar observation has also been made by Nicolau and Dupuy [9] for HgI_2 crystals. A possible explanation for the asymmetry of the bright contrast besides the dark points of Fig. 2 is an asymmetric distribution of radiative centers during the growth process. The regular dark lines in CL images of platelets and in some places of crystals (Figs. 2 and 4) are interpreted as dislocations lying in the basal plane.

After etching of the crystals the lens-shaped clusters of HgI_2 rich in impurities and/or Hg are revealed. Similar impurity and/or Hg-related clusters have often been reported [15–20] and systematically analyzed [21, 22]. Such clusters are seen (Fig. 5a and 5b) as round hillocks or as round pits. They often detach from the matrix, retaining their shape. They have different diameters, ranging from 0.2 to 5.0 μm. The cluster density and their mean diameters are not homogeneous in the crystals. Similar observations have also been made by Nicolau and Dupuy [9] in space-grown α-HgI_2 crystals by optical microscopic technique.

The appearance of three luminescence bands in HgI_2 at about the same wavelengths as the bands I, II and III of this work was first reported by Bube [23] from PL studies. The structure of the high-energy band has been found in low-temperature measurements to be very complex including exciton emissions and phonon replicas [24, 25]. Merz et al. [26] found that bands II and III are related to iodine deficiency and impurities, respectively. These three bands in our case have been observed all over the untreated samples. The total CL intensity decrease after KI treatment, can be partly due to light absorption in the residual etchant remaining on the surface and partly due to increase of surface roughness of the samples on etching. On the other hand the relative intensity changes of the bands show the effect of etching on the crystal defect structure. In particular, the sharp relative decrease of band II intensity can be explained by correlating this band with iodine deficiency in the samples. The sharp decrease of relative intensity of band II on KI treatment justifies the role of I vacancies on the emission of this band. As the samples were not washed after KI treatment, the reaction of KI continues for several days.

However, as the evaporation of I from the sample surfaces on keeping them in air [27] continues and with time the reaction of KI on the samples slows down, the increase of I_2/I_1 after about 10 days justifies our explanation .

Although the absolute intensity of band III decreased immediately after KI treatment, the relative intensity (I_3/I_1) increases with prolonged etching (Fig. 8). As stated above, the decrease of absolute intensity can be due to an absorption effect but the subsequent increase of relative intensity is an etching effect of the reacting KI on the sample. This band has been previously attributed to impurities [25] since it decreased when the starting HgI_2 powders were purified. The present results show that band III is not only due to extrinsic impurities but also to surface defects created by post-etching exposure. The increase of the relative intensity of band III even after several days of KI treatment supports the association of surface states on this band. As after some days of KI treatment, by keeping the samples in air, the surface becomes saturated with defect states, the relative intensity curve becomes flat.

In crystals an additional band appears at about 555 nm. Petroff et al. [12] have reported a CL band close to this wavelength in indented HgI_2 crystals and related it to the presence of dislocations generated during plastic deformation but not to grown-in dislocations. The CL images (Figs. 2 and 4) of the present work enable us to rule out the possibility that the 555 nm band is dislocation related. The dislocations lying in the basal plane appear in CL images of both platelets and crystals and do not show any correlation with the 555 nm luminescence. Although in crystals, immediately after etching, bands II and III almost vanish, the behavior of band III after prolonged etching is similar to the platelet case.

4 Conclusions

Growth instabilities in α-HgI_2 platelets cause the formation of terraces like steps and grooves on the surfaces. The basal plane dislocations are the common feature of HgI_2 platelets grown by the vapor transport method. In HgI_2 crystals grown by the vapor transport method, the basal plane dislocations can be observed only in some places. CL spectra show differences between platelets and crystals. KI etching suppresses deep level CL emissions in

crystals. The effect of prolonged KI treatment on HgI_2 platelets causes the reduction of luminous intensity of band II and creates some defect states on the surface attributed to band III.

Acknowledgements. U. Pal and N.V. Sochinski thank Spanish MEC for a post-doctoral research grant. This work has been supported by DGICYT (Project PB 93-1256) and CICYT (Project MAT92-0911-C02-01).

References

1. W.R. Willing: Nucl. Instrum. Methods **96,** 615 (1971)
2. H.L. Malm: IEEE Trans. NS-**19,** 263 (1972)
3. J.P. Ponpon, R. Stuck, P. Siffert: Nucl. Instrum. Methods **119,** 197 (1974)
4. H.L. Malm, T.W. Raudoff, M. Martina, K.R. Zanio: IEEE Trans. NS-**20,** 500 (1973)
5. R.B. James, D.K. Ottesen, D. Wong, T.E. Schlesinger, W.F. Schnepple, E. Ortale, L. Van de Berg: Nucl. Instrum. Methods A **283,** 188 (1989)
6. Z.L. Wu, J.L. Merz, L. Van de Berg, W.F. Schneppl: J. Lum. **24/25,** 197 (1981)
7. D. Wong, T.E. Schlesinger, R.B. James, E. Ortalc, L. Van de Berg, W.F. Schnepple: J. Appl. Phys. **64,** 2049 (1988)
8. I. Kh. Akopyan, B.V. Bondarenko, B.A. Karennov, B.V. Novikov: Sov. Phys.-Solid State **29,** 238 (1987)
9. Y.F. Nicolau, M. Dupuy: Nucl. Instrum. Methods A **283,** 355 (1989)
10. T. Kobayashi, J.T. Muheim, P. Waegli, E. Kaldis: J. Electrochem. Soc. **130,** 1183 (1983)
11. Y.F. Nicolau, M. Dupuy, Z. Kabosch: Nucl. Instrum. Methods A **283,** 149 (1989)
12. P.M. Petroff, Yu Peng Hu, F. Millstein: J. Appl. Phys. **66,** 2525 (1989)
13. M.D. Serrano, M.T. Santos, E. Dieguez, S.N. Toubektsis, M.F. Daviti, E.K. Polychroniadis: Cryst. Res. Technol. **29,** 525 (1994)
14. A. Cremades, F. Dominguez-Adame, J. Piqueras: J. Appl. Phys. **74,** 5726 (1993)
15. A. Mashimoto, F. Hayashi, T. Uematsu, Y. Moriyoshi: J. Mater. Sci. **1,** 4 (1982)
16. K. Tsukamoto, B. Van der Hock: J. Cryst. Growth **57,** 131 (1982)
17. Y.M. Gerasimov, G.I. Distler, V.M. Kanevsky, E.I. Kortukova, E.I. Suvorova, T.M. Okhrimenko, G.S. Belikova: Cryst. Res. Technol. **18,** 1283 (1983)
18. A.Y. Bunkin, A.A. Frolov: J. Cryst. Growth **69,** 131 (1984)
19. S.K. Behal, R.R. Chianelli, B.H. Kear: Mater. Lett. **3,** 381 (1985)
20. R. Rodriguez, M. Aguilo, J. Tejada: J. Cryst. Growth **47,** 518 (1979)
21. E. Bauser, H.P. Strunk: J. Cryst. Growth **69,** 561 (1984)
22. Y.C. Lu, E. Bauser: J. Cryst. Growth **71,** 305 (1985)
23. R.H. Bube: Phys. Rev. **106,** 703 (1957)
24. B.V. Novikov, M.M. Pimonenko: Sov. Phys.-Semicond. **46,** 671 (1972)
25. X.J. Bao, T.E. Schlesinger, R.B. James, C. Ortale, L. Van den Berg: J. Appl. Phys. **68,** 2951 (1990)
26. J.L. Merz, Z.L. Wu, L. Van den Berg, W.F. Schnepple: Nucl. Instrum. Methods **51,** 51 (1983)
27. R.B. James, X.J. Bao, T.E. Schlesinger, J.M. Markakis, A.Y. Cheng, C. Ortale: J. Appl. Phys. **66,** 2578 (1989)